

Quantum Interference Controlled Molecular Electronics

San-Huang Ke,¹ Weitao Yang,¹ and Harold U. Baranger²

¹Department of Chemistry, Duke University, Durham, NC 27708-0354

²Department of Physics, Duke University, Durham, NC 27708-0305

(Dated: August 29, 2008; published as Nano Lett. 8, 3257-3261 (2008))

Quantum interference in coherent transport through single molecular rings may provide a mechanism to control current in molecular electronics. We investigate its applicability by using a single-particle Green function method combined with *ab initio* electronic structure calculations. We find that the quantum interference effect (QIE) depends strongly on the interaction between molecular π states and contact σ states. It is masked by σ tunneling in small molecular rings with Au leads, such as benzene, due to strong π - σ hybridization, while it is preserved in large rings, such as [18]annulene, which then could be used to realize QIE transistors.

The use of single molecules as functional devices is the ultimate end of the ongoing trend toward miniaturization of electronic circuits^{1,2,3}. Despite significant progress made in the last decade, several issues still challenge the realization of molecular electronics, notably the sensitivity and control of molecule-lead contacts^{4,5,6}. Recently Cardamone et al.^{7,8} proposed a novel mechanism to control electron transport through single molecular rings: the current is determined by the degree of destructive or constructive quantum interference between the two paths around a symmetric molecule. Such interference can be controlled by a third terminal providing elastic scattering or dephasing. Their use of a quantum interference effect (QIE) in the completely coherent quantum regime builds on previous work in semiconductor nanostructures^{9,10} and molecular nanostructures^{11,12,13,14,15,16}. Since the QIE stems essentially from the symmetry of a molecular device, it should not be affected significantly by the structure of the molecule-lead contact. We present the first study of this novel mechanism in realistic *ab initio* calculations.

QIE controlled molecular electronics was proposed^{7,8} using a model calculation for a benzene ring in which only the π molecular states were considered. The connection between the leads and the molecular states was treated phenomenologically, and the possibility of induced structural relaxation was ignored. As these simplifications could have a big effect on the conductance, it is critical to investigate the validity of the QIE mechanism in realistic systems and to evaluate the factors affecting it.

In this paper, we investigate the QIE mechanism by performing quantum transport calculations for two molecular rings, one small – benzene – and one large – [18]annulene. We adopt a standard single-particle Green function method^{17,18} combined with *ab initio* electronic structure calculations in which all the above-mentioned factors are fully taken into account. Two different electrodes (leads) are studied: gold, which has π - σ molecule-lead coupling, and a metallic (5,5) carbon nanotube (CNT), which has strong π - π coupling.

Our calculations show that the survival of the QIE mechanism depends strongly on the interaction between the molecular π states and the contact σ states. It is masked by σ tunneling in the small benzene/Au system because of the strong π - σ hybridization, while it is preserved in the large [18]annulene/Au system, which then could be used to realize QIE transistors. With the CNT leads, we find that strong π - π molecule-lead coupling can modify significantly the QIE but does not

destroy it.

Our method for calculating electron transport through molecular junctions has been described in detail previously¹⁸; it combines a Landauer approach to transport with *ab initio* electronic structure methods^{19,20,21,22,23,24,25,26}. In particular, we use here density functional theory (DFT)²⁷ in the local density approximation (LDA), hybrid DFT in the version of B3LYP^{28,29}, and Hartree-Fock (HF) theory. Several energy functionals are used to make sure that the conclusions are generally valid, because to date no functional is completely accurate for transport calculations. Usually DFT-LDA and HF are the two extremes, the former overestimates and the latter underestimates the conductance³⁰. The wave functions are expanded using a Gaussian 6-311G** basis set for the C, H, and S atoms, and a CRENBs basis set for Au atoms³¹.

Practically, the lead-molecule-lead system is divided into three parts: left lead, right lead, and device region. The latter contains the molecule plus parts of the leads to accommodate the molecule-lead interaction (see structures below). The self-consistent DFT or HF Hamiltonian of the device region plus the self-energies of the two semi-infinite leads, $\Sigma_{L,R}(E)$, are used to construct a single-particle Green function, $\mathbf{G}_D(E)$, from which the transmission coefficient as a function of energy is calculated: $T(E) = \text{Tr}[\Gamma_L \mathbf{G}_D \Gamma_R \mathbf{G}_D^\dagger]$ where $\Gamma_{L,R}(E) = i[\Sigma_{L,R}(E) - \Sigma_{L,R}^\dagger(E)]$ is the coupling to the left or right lead. The conductance, G , then follows from a Landauer-type relation.

For the benzene ring, we consider only gold leads. The self-energy due to the Au within the leads is treated in the wide band limit (WBL) approximation: $\Gamma(E) = -\gamma \mathbf{I}$ with $\gamma = 3.0$ eV³². But note that the key molecule-lead coupling is included explicitly in the Hamiltonian because 9 Au atoms are included in the central device region. Since the density of states of gold is quite flat around the Fermi energy, the use of the WBL for Au atoms is reasonable. For the large [18]annulene ring, we consider gold leads as for benzene as well as (5,5) metallic carbon nanotube leads for which the self-energy is obtained by *ab initio* calculation of atomic leads. For all systems the atomic structure of the junction, including the molecule-lead separation, is optimized³³ by minimizing the atomic forces on atoms to be smaller than 0.02 eV/Å.

Let us start with the small system – the benzene ring in Fig. 1(a). All of the Au atoms included in the device region are shown; the WBL self-energy is applied to these atoms.

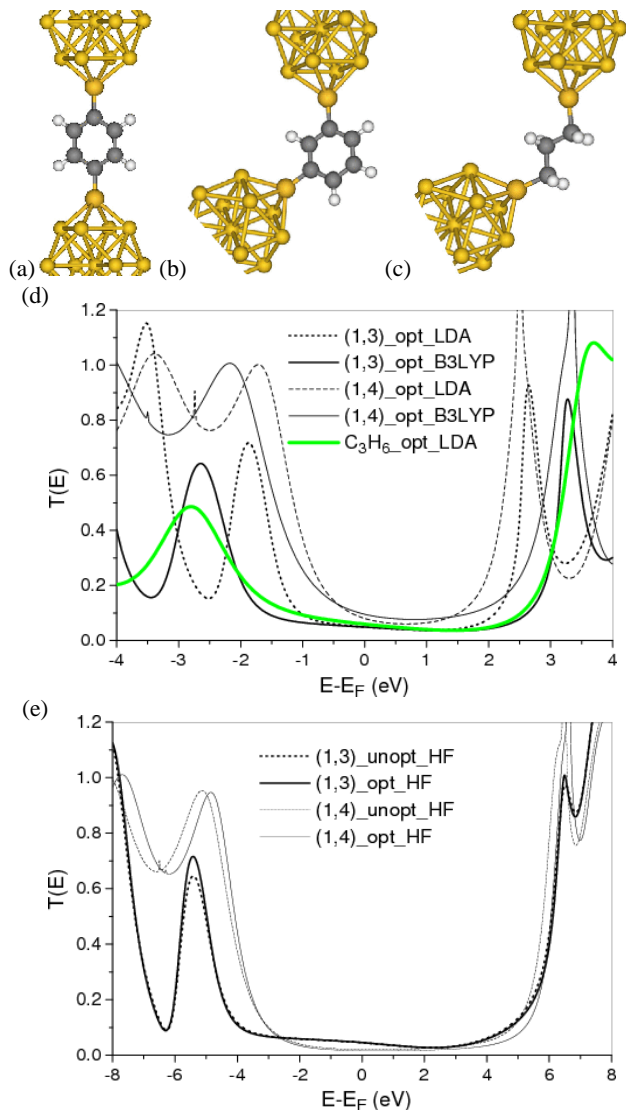


FIG. 1: (color online) Optimized structures of the Au-S-benzene-S-Au system (device region only) with (a) the (1,4) constructive and (b) the (1,3) destructive interference configurations. (c) The alkane configuration used for comparison. (d),(e) Transmission functions obtained with different energy functionals. For the HF calculation we consider cases both with and without the lead-induced molecular relaxation, as indicated. Note the absence of a clear difference between the (1,3) and (1,4) cases.

The S atom is situated on a hollow site. Two structural configurations are considered: (1,4) and (1,3) in Figs. 1(a) and 1(b), respectively. Configuration (1,4) has constructive interference in the all- π model (phase difference between the two paths around the ring is 0), while (1,3) has destructive interference (phase difference is π)^{7,8}. Still within the all- π model, the non-equilibrium many-body physics was subsequently studied in detail for these two configurations³⁴.

The transmission $T(E)$ found using several functionals is shown in Figs. 1(d) and (e). First, note that the transmission gap depends on the functional as expected: it increases in the order LDA, B3LYP, and HF. Also, the LDA equilibrium

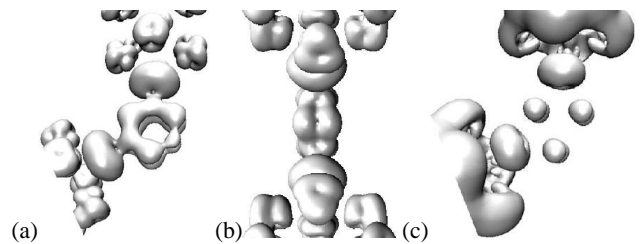


FIG. 2: Local density of states (LDOS) for the (1,3) benzene/Au system using LDA. (a) Top view and (b) side view for the energy window $[-2.5, -1.0]$ eV (HOMO resonance) in Fig. 1 (d). (c) Top view for the energy window $[-0.2, 0.2]$ eV. The influence of the σ bonds is clear in (a) and (b).

conductance for the (1,4) configuration is consistent with previous calculations^{35,36,37}, about $0.1G_0$. The key result here is the comparison between the (1,4) and the (1,3) configurations. The all- π model predicts that the (1,3) configuration has a transmission node at the Fermi energy due to total destructive interference^{7,8}. However, in our more realistic calculation, this transmission node does not occur. For LDA and B3LYP $G_{(1,3)}$ is smaller than $G_{(1,4)}$ by a factor of about 2; for HF the order is even reversed, $G_{(1,3)} > G_{(1,4)}$.

Several factors may destroy the perfect destructive interference present in the model of Refs. 7 and 8: (i) lead-induced structural relaxation which breaks the symmetry, (ii) the influence of the σ states, and (iii) beyond nearest-neighbor interactions which cause other paths. Let us first look at the effect of structural relaxation using the HF calculation: results for relaxed and unrelaxed structures are compared in Fig. 1(e). The effect on $T(E)$ is clearly minor. Because of the symmetry of the additional paths, the effect of (iii) should also be small. Thus, we conclude that factors (i) and (iii) are not important.

The first hint of the strong effect of σ hybridization comes from the difference between the transport gap in Fig. 1 and the HOMO-LUMO gap of an isolated benzene molecule. In LDA, for instance, the former is ~ 4.1 eV while the latter is 5.2 eV. This suggests that the HOMO and LUMO resonances may not be dominated by benzene π states. To check this, we plot in Fig. 2 the LDA local density of states (LDOS) both for the HOMO resonance (-2.5 eV to -1.0 eV) and for near the Fermi energy (-0.2 eV to 0.2 eV). Figs. 2(a) and (b) show that the HOMO resonance has large contributions from the contact Au-S states. Even in the benzene ring the σ character is remarkable. Because of this strong π - σ hybridization, transport near E_F consists largely of tunneling through the σ states rather than through the π -ring, as clearly shown by the LDOS around E_F in Fig. 2(c). To further examine this conclusion, we replace the benzene ring with a σ -bonded C_3H_6 molecule [Fig. 1(c)]. $T(E)$ in Fig. 1(d) (green line) shows that the conductance is very close to that of the (1,3) system, suggesting a similar transport mechanism. This shows directly that the conductance in the (1,3) configuration mainly comes from σ tunneling which masks the QIE effect.

Next we turn to the larger [18]annulene ring shown in Fig. 3. We consider two configurations which yield destructive interference in the π -only model^{7,8}, (1,7) and (1,9), and one

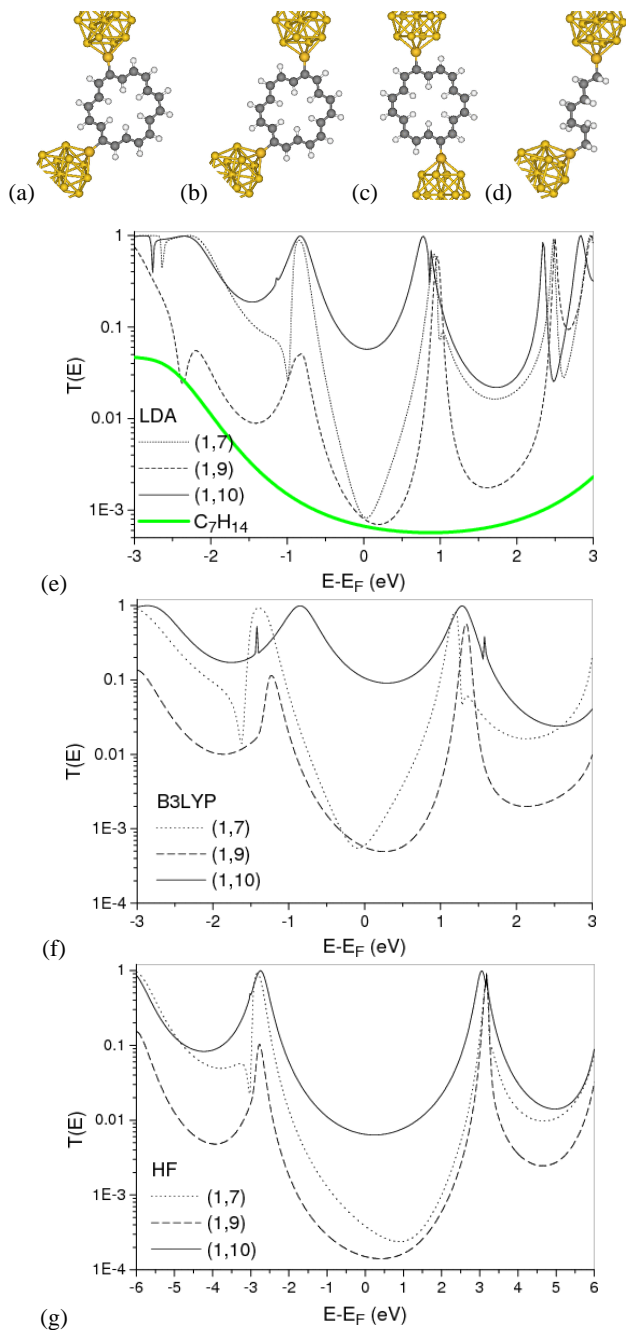


FIG. 3: (color online) Optimized structures for Au-S-[18]annulene-S-Au (device region only) with (a) (1,7), (b) (1,9), and (c) (1,10) lead configurations. (d) The alkane structure used for comparison. Transmission functions are given in (e) LDA, (f) B3LYP, and (g) HF. Note the clear difference between configurations with destructive and constructive interference.

constructive configuration, (1,10). From the $T(E)$ given by LDA, B3LYP, and HF one sees the same trend in the transport gap and in the equilibrium conductance: the smallest conductance is given by HF with the largest gap, which is about one order of magnitude smaller than the LDA result, in agreement with a previous result for other long-chain molecules³⁰. The key feature here is that the conductance for (1,7) and (1,9) is

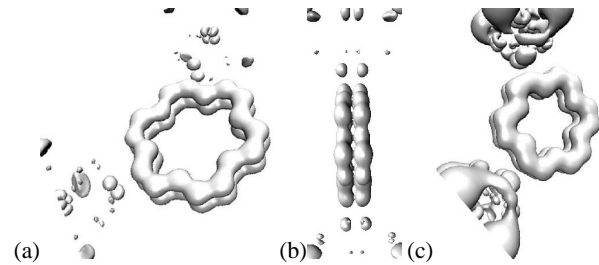


FIG. 4: LDOS for the (1,7) [18]annulene/Au system from LDA. (a) Top view and (b) side view for the energy window [-1.0, -0.2] eV (HOMO resonance) in Fig. 3 (e). (c) Top view for the energy window [-0.2, 0.2] eV (Fermi energy). The π -orbital signature is clear.

much smaller than that for the (1,10), by about two orders of magnitude. *This indicates that, in contrast to benzene, the ideal destructive interference is largely preserved.*

To understand this, we show in Fig. 4 the LDA LDOS near both the HOMO resonance (-1.0 eV to -0.2 eV) and the Fermi energy (-0.2 eV to 0.2 eV). One sees that the HOMO resonance is dominated by the [18]annulene π states, and transport near the Fermi energy is basically through the π -ring. Because of the near perfect destructive interference of the π transmission^{7,8}, the residual conductance should come from σ -bond tunneling. To check this, we replace the [18]annulene ring with a σ -bonded C_7H_{14} chain [see Fig. 3(d)]. The $T(E)$ [green line in Fig. 3(e)] yields a conductance very close to that of (1,7), confirming our view.

How to understand the difference in behavior between the small benzene ring and the large [18]annulene ring? The answer lies in the energies of the molecular levels. In LDA, for example, the energy of benzene π states (HOMO) is -6.5 eV which is in the energy window of the Au-S bonding at the contact, from -7.0 to -5.7 eV. The larger size of [18]annulene means that its π states (HOMO) are higher in energy, at -5.0 eV, which is well above the energy window of the Au-S bonding. Consequently, in [18]annulene, the π orbital becomes the frontier orbital which therefore dominates transport.

From this picture one can see that the advantage of using larger conjugated molecules is two-fold: First, the resulting π -dominated transport preserves the simple quantum interference effects. Second, the longer length suppresses σ tunneling, leading to a larger on/off ratio.

While Au electrodes have some advantages, they have a severe disadvantage as well: the contact transparency is poor (despite the strong chemical bond), leading to a small equilibrium conductance even in the case of constructive interference. For a more favorable case with strong coupling near the Fermi energy, we use a metallic (5,5) carbon nanotube as a lead, connecting to the molecule through a 5-member-ring³⁸. The optimized structures are shown in Fig. 5 for the (1,10) and (1,7) configurations; both have a co-planar structure which provides overall conjugation and thus strong molecule-lead π - π coupling.

The strong molecule-lead coupling leads to a metal-induced gap state traveling into the molecule³⁸. For short conjugated molecules, the two states originating from the two leads will

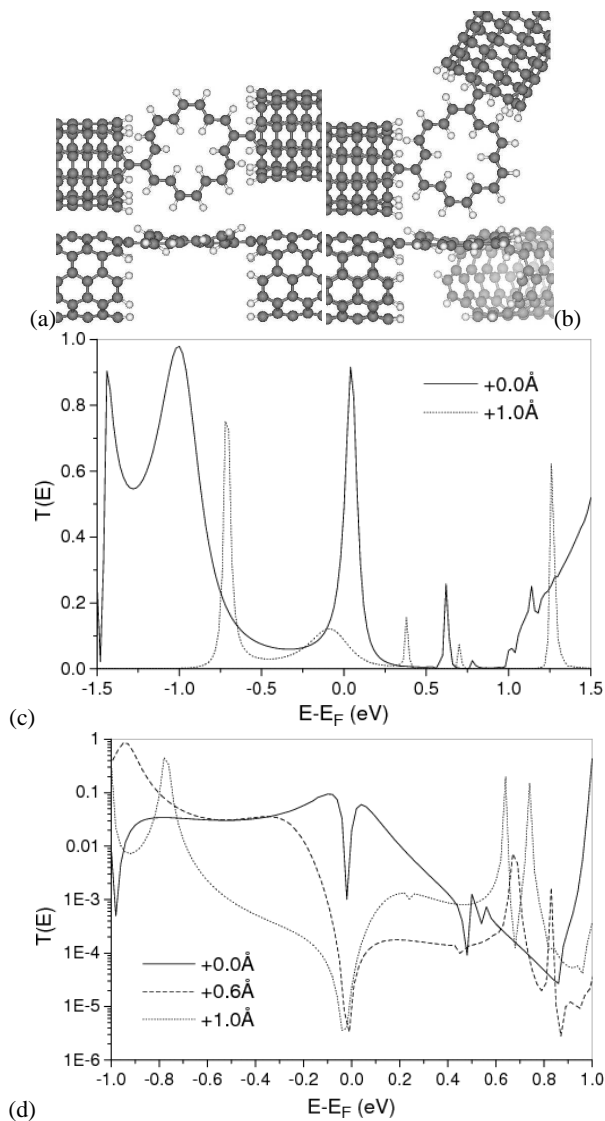


FIG. 5: Optimized structures of the 5-member-ring-connected (5,5)CNT-[18]annulene-(5,5)CNT junctions with the lowest total energies: (a) constructive (1,10) and (b) destructive (1,7) configurations. Their transmission functions for different molecule-lead separations (indicated in the legend) are given in (c) and (d), respectively. Note the resonance peak around the Fermi energy in (c) and the anti-resonance peak in (d).

meet in the molecule, causing a resonance peak in $T(E)$ around E_F . This is just what we see in Fig. 5(c) for the constructive (1,10) configuration. [For $T(E)$ here, we do not use the WBL, but rather find the lead self-energy from an atomistic *ab initio* calculation.] The resonance peak decays as we increase artificially the molecule-lead separation (weaken the coupling), as shown in Fig. 5(c). For the destructive (1,7) configuration [Fig. 5(d)], an *anti-resonance* peak appears at E_F , indicating that the destructive interference applies in the strong coupling limit to the metal-induced gap state (though the anti-resonance is rather narrow). For larger molecule-lead separation (weaker coupling), the anti-

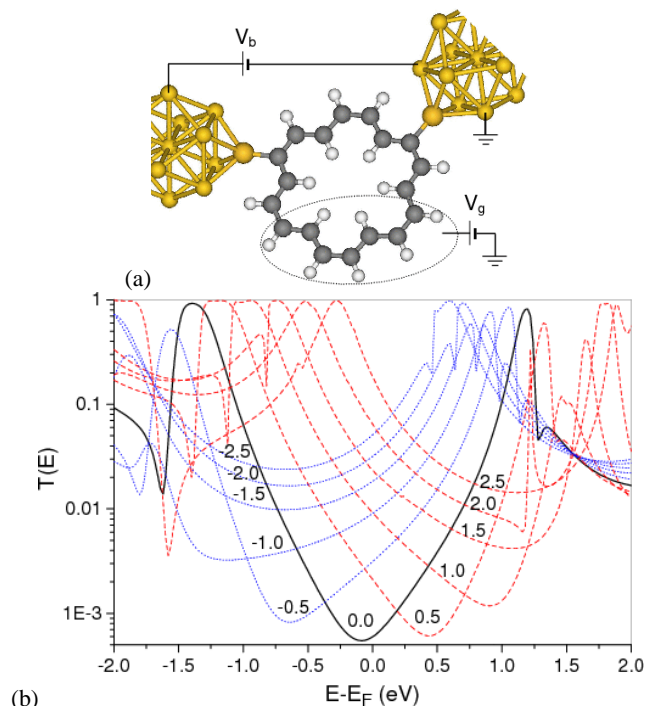


FIG. 6: (color online) (a) A schematic drawing of a [18]annulene-based field-effect QIE transistor. The source-drain current is controlled by the gate voltage V_g which causes elastic scattering in the gated region. The transmission functions for zero bias ($V_b=0$) and different V_g are given in (b).

resonance becomes wider and deeper; thus, the molecule-lead coupling affects significantly the quantum interference but does not destroy it. Note that here the metal-induced gap state leads to a much larger constructive conductance and a larger on/off ratio compared with the case of Au leads.

The effective destructive quantum interference can be used to control electric current through single molecular devices. To demonstrate this explicitly, we propose a model device structure, shown in Fig. 6, using a Au-S-[18]annulene-S-Au (1,7) junction, where a local gate potential (due to an STM tip, for instance) is applied to part of the molecular ring, which will destroy partially the destructive interference because of the additional scattering, depending on the gate voltage, V_g . The calculation is carried out using the B3LYP functional. The computational techniques for transport in the presence of a local gate potential shift has been described previously³⁹. Fig. 6(b) shows the transmission functions for different gate voltages. One can see that a small gate voltage can modify significantly the transmission function of the device, both shifting and greatly distorting the transmission valley. Most importantly, a small gate voltage can increase the equilibrium conductance by up to three orders of magnitude – a good behavior for field-effect QIE transistors.

We would like to finish this Letter with a comment about the effect of molecular thermal vibration on QIE. For non-interference-related electron transport through single molecules which are not very long, molecular vibration should have a very small effect on the I - V characteristics be-

cause the transport is basically ballistic as long as extremely soft vibrational modes (which may lead to conformational changes) are absent. For QIE, the relevant vibrational modes are those which change the length difference between the two paths. These modes therefore involve changing the C-C bond length and have very high frequencies. As a result, the effect

of molecular vibration on QIE for room temperature can be expected to be small.

We thank Charles Stafford for a series of valuable conversations. This work was supported in part by the NSF (DMR-0506953).

-
- ¹ Nitzan, A.; Ratner, M. A. *Science* **2003**, *300*, 1384-1389.
- ² Tao, N. J. *Nature Nanotech.* **2006**, *1*, 173-181.
- ³ Koentopp, M.; Chang, C.; Burke, K.; Car, R. *J. Phys.: Condens. Matter* **2008**, *20*, 083203 (21pp).
- ⁴ Venkataraman, L.; Klare, J. E.; Tam, I. W.; Nuckolls, C.; Hybertsen, M. S.; Steigerwald, M. L. *Nano Lett.* **2006**, *6*, 458-462.
- ⁵ Basch, H.; Cohen, R.; Ratner, M. A. *Nano Lett.* **2005**, *5*, 1668 - 1675.
- ⁶ Ke, S.-H.; Baranger, H. U.; Yang, W. *J. Chem. Phys.* **2005**, *122*, 074704.
- ⁷ Cardamone, D. M.; Stafford, C. A.; Mazumdar, S. *Nano Lett.* **2006**, *6*, 2422 - 2426.
- ⁸ Stafford, C. A.; Cardamone, D. M.; Mazumdar, S. *Nanotechnology* **2007**, *18*, 424014 - 424019.
- ⁹ Sols, F.; Macucci, M.; Ravaioli, U.; Hess, K. *Appl. Phys. Lett.* **1989**, *54*, 350.
- ¹⁰ Goodnick, S.; Bird, J. *IEEE Trans. Nanotech.* **2003**, *2*, 368-385.
- ¹¹ Sautet, P.; Joachim, C. *Chem. Phys. Lett.* **1988**, *153*, 511.
- ¹² Baer, R.; Neuhauser, D. *J. Am. Chem. Soc.* **2002**, *124*, 4200.
- ¹³ Yaliraki, S. N.; Ratner, M. A. *Ann. N.Y. Acad. Sci.* **2002**, *960*, 153.
- ¹⁴ Hettler, M. H.; Wenzel, W.; Wegewijs, M. R.; Schoeller, H. *Phys. Rev. Lett.* **2003**, *90*, 076805.
- ¹⁵ Stadler, R.; Forshaw, M.; Joachim, C. *Nanotechnology* **2003**, *14*, 138.
- ¹⁶ Stadler, R.; Thygesen, K. S.; Jacobsen, K. W. *Nanotechnology* **2005**, *16*, S155-S160.
- ¹⁷ Haug, H.; Jauho, A.-P. *Quantum Kinetics in Transport and Optics of Semiconductors*; Springer-Verlag: Berlin, 1996.
- ¹⁸ Ke, S.-H.; Baranger, H. U.; Yang, W. *Phys. Rev. B* **2004**, *70*, 085410.
- ¹⁹ DiVentra, M.; Pantelides, S. T.; Lang, N. D. *Phys. Rev. Lett.* **2000**, *84*, 979 - 982.
- ²⁰ Taylor, J.; Guo, H.; Wang, J. *Phys. Rev. B* **2001**, *63*, 245407.
- ²¹ Damle, P. S.; Ghosh, A. W.; Datta, S. *Phys. Rev. B* **2001**, *64*, 201403(R).
- ²² Xue, Y.; Datta, S.; Ratner, M. A. *Chem. Phys.* **2002**, *281*, 151-170.
- ²³ Brandbyge, M.; Mozos, J.-L.; Ordejón, P.; Taylor, J.; Stokbro, K. *Phys. Rev. B* **2002**, *65*, 165401.
- ²⁴ Louis, E.; Vergés, J. A.; Palacios, J. J.; Pérez-Jiménez, A. J.; SanFabián, E. *Phys. Rev. B* **2003**, *67*, 155321 (5 pages).
- ²⁵ Rocha, A. R.; Garcia-Suarez, V.; Bailey, S. W.; Lambert, C. J.; Ferrer, J.; Sanvito, S. *Phys. Rev. B* **2006**, *73*, 085414.
- ²⁶ Arnold, A.; Weigend, F.; Evers, F. *J. Chem. Phys.* **2007**, *126*, 174101.
- ²⁷ Parr, R. G.; Yang, W. *Density-Functional Theory of Atoms and Molecules*; Oxford University Press: New York, 1989.
- ²⁸ Becke, A. D. *J. Chem. Phys.* **1993**, *98*, 5648.
- ²⁹ Lee, C.; Yang, W.; Parr, R. G. *Phys. Rev. B* **1988**, *37*, 785.
- ³⁰ Ke, S.-H.; Baranger, H. U.; Yang, W. *J. Chem. Phys.* **2007**, *126*, 201102.
- ³¹ NWChem, A Computational Chemistry Package for Parallel Computers, Pacific Northwest National Lab, Richland, Washington, USA (2003).
- ³² This value is chosen by almost reproducing the transmission functions of Au-conjugated molecule-Au junctions, obtained with *ab initio* calculated self-energies for the semi-infinite leads. A change in γ of up to ± 2 eV will cause quantitative difference in the transmission function but does not alter the qualitative conclusion.
- ³³ The structure optimization calculations are performed by using a numerical basis set of double zeta plus polarization (DZP)⁴⁰ combined with the use of optimized Troullier-Martins pseudopotentials⁴¹. The generalized gradient approximation in the version of PBE⁴² is adopted for the exchange and correlation.
- ³⁴ Begemann, G.; Darau, D.; Donarini, A.; Grifoni, M. *Phys. Rev. B* **2008**, *77*, 201406.
- ³⁵ Xue, Y.; Datta, S.; Ratner, M. A. *J. Chem. Phys.* **2001**, *115*, 4292-4299.
- ³⁶ Xue, Y.; Ratner, M. A. *Phys. Rev. B* **2003**, *68*, 115407-115418.
- ³⁷ Ke, S.-H.; Baranger, H. U.; Yang, W. *J. Chem. Phys.* **2005**, *123*, 114701.
- ³⁸ Ke, S.-H.; Baranger, H. U.; Yang, W. *Phys. Rev. Lett.* **2007**, *99*, 146802.
- ³⁹ Ke, S.-H.; Baranger, H. U.; Yang, W. *Phys. Rev. B* **2005**, *71*, 113401.
- ⁴⁰ Soler, J. M.; Artacho, E.; Gale, J. D.; Garcia, A.; Junquera, J.; Ordejón, P.; Sanchez-Portal, D. *J. Phys.: Condens. Matter* **2002**, *14*, 2745-2779.
- ⁴¹ Troullier, N.; Martins, J. L. *Phys. Rev. B* **1991**, *43*, 1993-2006.
- ⁴² Perdew, J. P.; Burke, K.; Ernzerhof, M. *Phys. Rev. Lett.* **1996**, *77*, 3865-3868.